

1 **GENERALIST: An efficient generative model for protein sequence families**

2 Hoda Akl^{1*}, Brooke Emison¹, Xiaochuan Zhao¹, Arup Mondal², Alberto Perez², and Purushottam D.
3 Dixit^{1,3,4,5,*}

4 ¹Department of Physics, University of Florida, Gainesville, FL 32603

5 ²Department of Chemistry, University of Florida, Gainesville, FL 32611

6 ³Department of Chemical Engineering, University of Florida, Gainesville, FL 32603

7 ⁴UF Genetics Institute, University of Florida, Gainesville, FL 32608

8 ⁵UF Health Cancer Center, University of Florida, Gainesville, FL 32610

9 *Email: Purushottam Dixit: pdixit@ufl.edu, Hoda Akl: hodaakl@ufl.edu

10
11 **Abstract**

12 Generative models of protein sequence families are an important tool in the repertoire of
13 protein scientists and engineers alike. However, state-of-the-art generative approaches face
14 inference, accuracy, and overfitting-related obstacles when modeling moderately sized to large
15 proteins and/or protein families with low sequence coverage. To that end, we present a simple
16 to learn, tunable, and accurate generative model, GENERALIST: *GENERAtive nonLInear tenSor-*
17 *factorizaTion* for protein sequences. Compared to state-of-the-art methods, GENERALIST
18 accurately captures several high order summary statistics of amino acid covariation.
19 GENERALIST also predicts conservative local optimal sequences which are likely to fold in stable
20 3D structure. Importantly, unlike other methods, the density of sequences in GENERALIST-
21 modeled sequence ensembles closely resembles the corresponding natural ensembles.
22 GENERALIST will be an important tool to study protein sequence variability.

23

24

25

26

27

28

29

30

31

32

33

34

35

36

37

38

39

40

41

42

43

44

45

46

47

48

49 **Introduction**

50

51 Advances in *omics* technologies allow us to investigate sequences of evolutionarily related
52 proteins from several different organisms. Surprisingly, even when the function and structure
53 are conserved, sequences within protein families can vary substantially¹. This variability is
54 governed by a combination of factors, including protein stability², interaction partners³, and
55 function⁴. Therefore, it is not feasible to rationalize observed variation in protein sequences
56 using bottom-up mechanism driven models.

57

58 To understand the forces that constrain protein sequence variability and to identify new protein
59 sequences that perform desired functions, we need methods to sample sequences that are
60 likely to result in functional proteins⁵. Generative models of protein families that use multiple
61 sequence alignments (MSAs) are one such approach. These models attempt to learn the
62 covariation between amino acids across different positions and model a distribution over the
63 sequence space that captures aspects of the observed covariation. The Potts model is one of the
64 most popular generative models of protein families⁶. Potts model is a maximum entropy model
65 constrained to reproduce positional amino acid frequencies and position-position pair
66 correlations. Even though only 1- and 2-site frequencies are constrained, the model can
67 reproduce higher order covariation statistics⁷. The model is easy to interpret, as it assigns an
68 energy to sequences. In addition to modeling covariance between amino acid positions, Potts
69 models have also been used to rationalize effects of mutations on fitness⁸, and to predict
70 physical contacts between residues⁷.

71

72 However, there are significant issues with the Potts model. The associated numerical inference
73 is computationally inefficient⁹, limiting their application to small proteins and protein domains
74 ($L \sim 100$ residues). In comparison, median protein size in many organisms including humans is
75 much larger (~ 350 residues)¹⁰. Due to the numerical inefficiencies in inference, there is no
76 realistic way to tune the model beyond one- and two- position moments, for example, by
77 incorporating multi-position correlations. Moreover, the model has many hyperparameters,
78 including pseudocounts¹¹ for unobserved amino acids and parameters related to phylogenetic
79 reweighting¹². How model predictions depend on these hyperparameters is not always clear.
80 Finally, as we will show below, the Potts model does not reproduce statistics related to the

81 density of sequences and result in highly unnatural optimal sequences. Field theoretic
82 approaches¹³ can systematically generalize the Potts model by incorporating higher order
83 epistasis. However, these models can only be trained on very small sequences. Another recent
84 generalization that combines elements of autoregressive modeling and the Potts model; the
85 autoregressive DCA model¹⁴, addresses the numerical issues associated with the Potts model.
86 However, as we show below, this approach does not reproduce statistics related to the density
87 of sequences and overfits the data when modeling families of large proteins with small MSAs.

88

89 Deep generative (DG) models are a potential alternative¹⁵ to Potts models for realistically sized
90 proteins. However, DG models require large amounts of training data and lack interpretability.
91 While sequencing advances have led to large MSAs, especially for bacterial protein families,
92 many human proteins only exist in mammals and other higher order organisms where the MSA
93 sizes are currently limited by the number of sequenced genomes and ultimately by the total
94 number of mammalian species¹⁶. Neural network architectures are notorious for being over
95 parametrized, including several hyperparameters for training the networks. Finally, as we show
96 below, NN-based generative models may not necessarily improve in accuracy with the
97 increasing complexity of the architecture.

98

99 Therefore, there is an urgent need for efficient, tunable, and accurate generative models. To
100 that end, we present here GENERALIST: *GENERative nonLInear tenSor-factorizaTion*-based
101 model for protein sequences and other categorical data. In GENERALIST, we model individual
102 protein sequences in the data as arising from a sequence-specific Gibbs-Boltzmann
103 distribution^{17,18}. The energies of the distribution are shared across all sequences and the
104 temperatures are assigned in a sequence-specific manner. The modeler only specifies
105 complexity of the model (see below), and both the energies and the temperatures are inferred
106 directly from the data. The temperatures embed individual sequences in a latent space which
107 can be tuned to achieve a user-desired tradeoff between the novelty of generated sequences
108 and the accuracy of the ensemble in reproducing properties of the natural MSA.

109

110 We use GENERALIST to model sequence variability in proteins that span multiple kingdoms of
111 life, alignment sizes, and sequence lengths. We compare the performance of GENERALIST with
112 three other generative models, the Potts model (referred to as adabmDCA⁹), the autoregressive

113 DCA model (referred to as ArDCA¹⁴), and a variational autoencoder-based model (referred to as
 114 VAE¹⁹). We show that compared to these other models, GENERALIST captures higher order
 115 statistics of amino acid covariation across sequences. GENERALIST also predicts conservative
 116 local optima that are likely to fold in stable three-dimensional structures. Importantly, the
 117 ensemble of sequences generated using GENERALIST most accurately represents the density of
 118 sequences observed in nature. We believe that GENERALIST will be an important tool to model
 119 protein sequences and other categorical data.

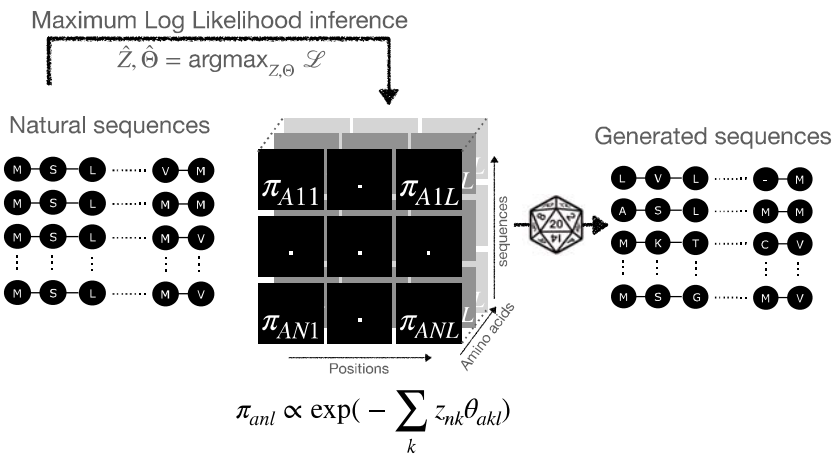
120

121 **Results**

122

123 **The Mathematical formalism of GENERALIST**

124



125

126 **Figure 1.** Schematic of the GENERALIST approach. Sequences are modeled as arising from their own
 127 Gibbs-Boltzmann distributions over categorical variables. The inferred probabilities are used to generate
 128 new sequences.

129

130 In GENERALIST (Figure 1), we start with a one-hot encoded representation of a multiple
 131 sequence alignment of N sequences of length L ; $\sigma_{nla} = 1$ if the amino acid at position l in the
 132 protein sequence indexed n has the identity a . Sequences are modeled as arising from their
 133 own Gibbs-Boltzmann distribution^{17,18}:

$$\pi_{anl} = \frac{1}{\Omega_{nl}} \exp\left(-\sum_{k=1}^K z_{nk} \theta_{akl}\right). \quad (1)$$

134

135 In Eq. (1), z_{nk} are sequence-specific inverse temperature-like quantities (latent space
 136 embeddings), θ_{akl} are position and amino acid dependent variables, and Ω_{nl} is the partition
 137 function that normalizes the probabilities. We can write down the total log-likelihood of
 observing the data:

$$\mathcal{L} = \sum_{n,l,a} \sigma_{anl} \log \pi_{anl} = - \sum_{n,l,a,k} \sigma_{anl} z_{nk} \theta_{akl} - \sum_{n,l} \log \Omega_{nl}. \quad (2)$$

138 The gradients of the log likelihood with respect to position- and amino-acid dependent
139 parameters θ_{akl} and z_{nk} are analytical. The parameters are simultaneously inferred using
140 maximum likelihood inference. Once the parameters are inferred, sequences can be sampled in
141 the vicinity of any sequence in the MSA using probabilities inferred in Eq. (1).

142

143 Below, we present our results for two proteins: Bovine Pancreatic Trypsin Inhibitor or BPT1, a
144 small protein domain comprising ~ 50 amino acids with a large MSA of ~ 16000 sequences and
145 epidermal growth factor receptor or EGFR, a large protein comprising ~ 1000 amino acids with
146 a small MSA of ~ 1000 sequences. In the SI, we show our analyses for dihydrofolate reductase
147 or DHFR (~ 160 amino acids, ~ 7000 sequences in the MSA), p53 (~ 350 amino acids, ~ 800
148 sequences in the MSA), and mammalian target of rapamycin or mTor (~ 2500 amino acids,
149 ~ 500 sequences in the MSA). Details of model training can be found in SI Section 1.

150

151 **Choosing the optimal latent space dimension in GENERALIST**

152

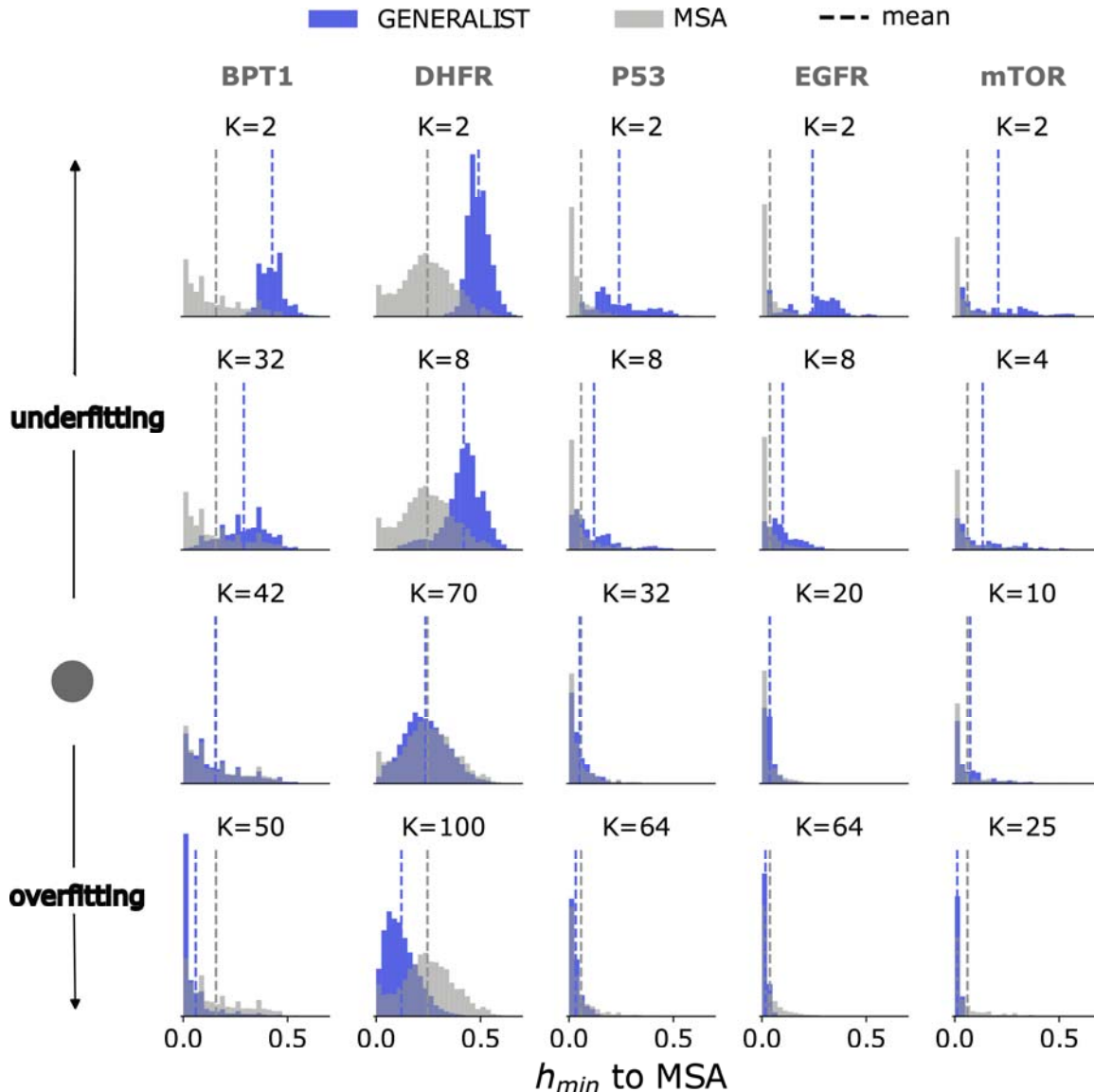
153 GENERALIST is a latent space model. Increasing latent space dimension typically improves the
154 ability of the generated ensemble to accurately capture summary statistics of the data (for
155 example, amino acid frequencies and covariation). At the same time, a high dimensional latent
156 space can result in a generated ensemble that is nearly identical to the natural one; trivially
157 reproducing all statistics but failing to generate new sequences. Therefore, a common challenge
158 with latent space models is selecting an appropriate dimension to avoid overfitting.

159

160 GENERALIST offers a natural way of evaluating overfitting. We computed for each generated
161 sequence the fractional Hamming distance (fraction of positions that have a different amino
162 acid) to the closest natural sequence (blue distributions in Figure 2, SI Section 2). We compared
163 these distributions to the distribution of nearest neighbor distances within the natural
164 ensembles (gray distributions in Figure 2). For an overfit ensemble, the distribution will peak
165 sharply at zero; implying that generated sequences are nearly identical to natural ones. In Figure
166 2, we show these distance distributions for GENERALIST ensembles trained with different latent
167 space dimensions. When the latent space dimension is low, GENERALIST ensembles comprise
168 sequences that are on average different from the natural sequences (as quantified by the mean

169 fractional Hamming distance to the closest natural sequence, blue bar). However, the
170 ensembles tend towards overfitting with higher latent space dimension, as seen in the leftward
171 shift in the distribution of distances to the nearest natural neighbor.

172



173

174 **Figure 2.** The distribution of distances to the nearest natural sequence for multiple latent space
175 dimensions. For each protein and a given latent space dimension, an *in silico* ensemble was generated
176 using GENERALIST. For each generated sequence, the minimum fractional Hamming distance to the
177 natural ensemble was evaluated (blue). The same calculation was repeated for natural sequences (gray).
178 The dashed vertical lines represent the means of the distributions. The gray disc on the left indicates the
179 optimal latent space dimension for each protein.

180

181 In the middle, we find the optimal latent space dimension as the one that matches the average
182 separation between nearest neighbors in natural sequences (dashed gray line) and the average

183 separation between sequences in the generated ensemble and the nearest natural neighbor
184 (dashed blue line). For the rest of the analyses, we choose this optimal dimension for the
185 studied proteins. Notably, variational autoencoders lend themselves to a latent space
186 description as well. Yet, we observed that ensembles generated using VAEs did not exhibit a
187 systematic trend towards overfitting when the latent space dimension was increased (SI Figure
188 1).

189

190 **GENERALIST reproduces high order summary statistics of natural sequences**

191

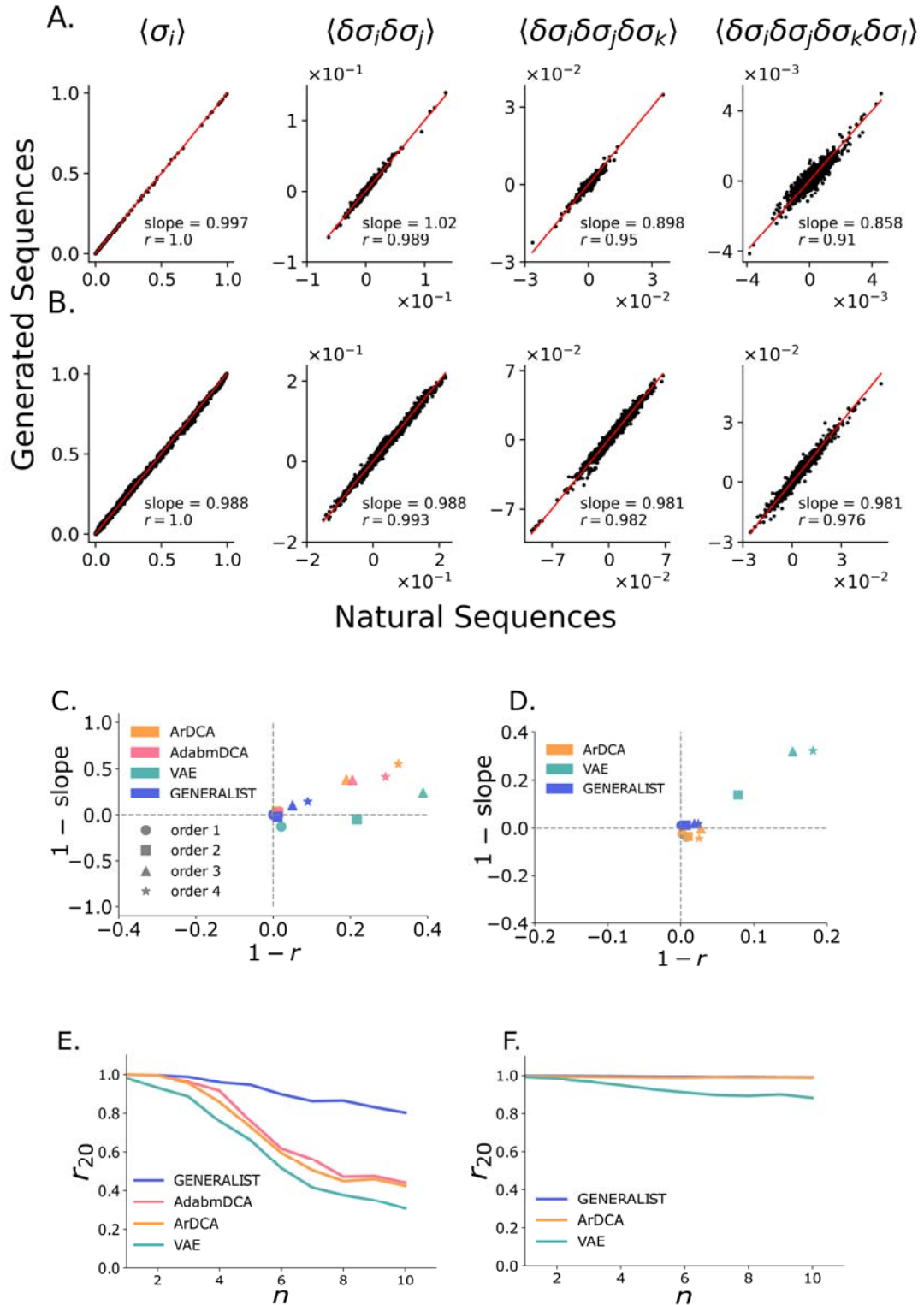
192 A key metric to evaluate the accuracy of generative models is their ability to reproduce
193 summary statistics on the sequences (SI Section 3). In Figures 3A and 3B, we show for BPT1 and
194 EGFR that GENERALIST accurately reproduces amino acid frequencies and mean removed
195 positional correlations up to order 4. Notably, as seen in Figure 3C and 3D (SI Figure 2), while
196 adabmDCA, ArDCA, and VAE-based predictions of positional frequency statistics correlate
197 strongly with those observed in the natural sequences (SI Section 4); these methods typically
198 under-predict these statistics (quantified by the slope of the best fit line).

199

200 Next, we investigated the ability of the generated ensembles to reproduce very high order
201 summary statistics. Most amino acid combinations of order higher than 4 are rarely found in
202 natural MSAs. We therefore used a recently introduced metric r_{20} that measures the average
203 Pearson correlation between the occurrence frequency of the top 20 amino acid combinations
204 of any given order²⁰. In Figure 3E and 3F (SI Figure 3), we show that GENERALIST accurately
205 captures co-occurrence frequencies of the most frequent amino acid combinations up to order
206 10. The ability of GENERALIST to capture these higher order statistics did not depend on
207 restricting our attention to the top 20 amino acid combinations (SI Figure 4). In comparison,
208 adabmDCA, ArDCA, and VAEs led to less accurate predictions about higher order correlations
209 when the MSAs were large (BPT1 in the main text and DHFR in the SI). Importantly, the
210 ensembles generated using VAEs did not exhibit a systematic trend toward more accurate
211 predictions when the latent space dimension was increased (SI Figure 1). Finally, ArDCA could
212 capture higher order positional correlations for large proteins with small MSAs (Figure 3F, SI
213 Figure 3). However, as we will show below, this was due to overfitting.

214

215 These results conclusively show that GENERALIST-based sequence ensembles retain positional
 216 correlation information of arbitrarily high orders observed in naturally occurring sequences for
 217 large proteins as well as for proteins with very small MSAs.



218

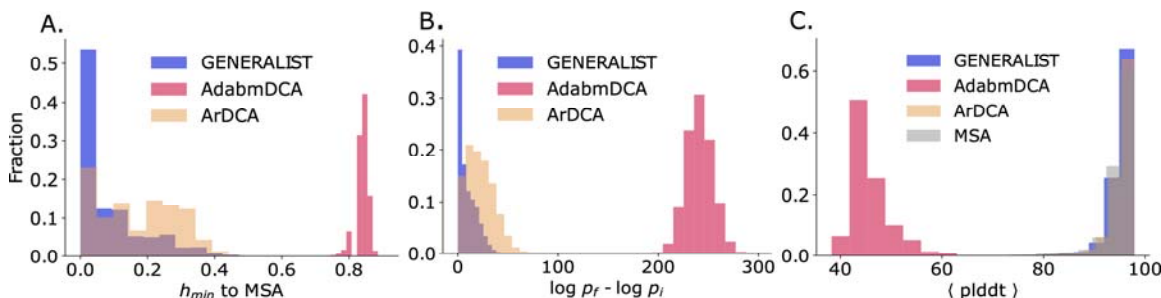
219 **Figure 3. Panels A and B.** Comparison of amino acid frequencies, mean removed pair, three and four body
220 correlations calculated from GENERALIST-generated in silico ensembles (y-axis) and the natural sequences
221 (x-axis) for BPT1 (panel A) and EGFR (panel B). **Panels C and D.** 1 – Pearson correlation coefficient versus 1
222 – slope of the best fit line for the comparison between amino acid frequencies, mean removed pair, three
223 and four body correlations for GENERALIST, ArDCA, adabmDCA, and VAEs shown for BPT1 (panel C) and
224 EGFR (panel D). **Panels E and F.** The average Pearson correlation coefficient between frequencies of top
225 20 amino acid combinations of order n (x-axis) averaged across different combinations (y-axis) for
226 GENERALIST, ArDCA, adabmDCA, and VAEs shown for BPT1 (panel E) and EGFR (panel F).

227

228 **GENERALIST finds conservative optimal sequences**

229

230 A key feature of generative models is the ability to assign probabilities to arbitrary sequences
231 and therefore find local sequence optima (sequences corresponding to the local maximum of
232 the probability). The local optima inform us about the local structure of the inferred sequence
233 space energy landscape and their relationship to naturally occurring sequences. For example, if
234 the generative models are purely data-driven, that is, if they do not incorporate any information
235 about structure/function/fitness, it may be desirable that the local optima are in the vicinity of
236 natural sequences.



237

238 **Figure 4. Panel A.** The distribution of distances to the nearest natural neighbor from sequences optimized
239 using GENERALIST, ArDCA, and adabmDCA modeled probabilities. **Panel B.** The log-fold improvement in
240 probabilities between the starting sequence and the local optimum. **Panel C.** Sequence-averaged plddt
241 scores for AlphaFold2 predicted structures for the locally optimum sequences.

242

243 To test the relationship between local optimum sequences and natural sequences, we use
244 GENERALIST, adabmDCA, and ArDCA to obtain locally optimal sequences. VAE was not included
245 because VAEs involve a nonlinear transformation from the latent space to the sequence space
246 and therefore the probability in the sequence space is difficult to calculate.

247

248 We obtained local minima in adabmDCA and ArDCA using a random search (SI Section 5). Briefly,
249 we start from sequences in the natural MSA and randomly mutated amino acids while only
250 accepting mutations that improve sequence probability as evaluated by the model. Multiple
251 iterations of this operation lead to local optimum sequences. The local optimum sequences
252 predicted by GENERALIST were obtained by finding the highest probability sequence

253 corresponding to the latent space embedding of natural sequences. This analysis was only
254 performed on BPT1 where all three models could be trained in a reasonable time.

255
256 As seen in Figure 4A, adabmDCA generates locally optimal sequences that differed by a
257 staggering 84% from the closest naturally occurring sequence neighbor. These optimal
258 sequences were predicted to be significantly better compared to the starting natural sequences,
259 with an average improvement by ~ 110 fold in probability at each position (with a total average
260 increase in probability by a factor of $\sim 5 \times 10^{104}$ when considering the entire sequence) (Figure
261 4B, measured by log odds ratio). These local minima in the Potts model that do not resemble
262 any natural sequences are reminiscent of the unwanted spurious minima in Hopfield networks²¹.
263 Compared to adabmDCA, ArDCA generated local optimal sequences that were significantly more
264 conservative (on an average, 17% difference compared to 84%) (Figure 4A). The optimal
265 sequences were also predicted to be a relatively modest improvement over the starting natural
266 sequence with an improvement by ~ 1.5 fold in probability at each position with a total average
267 increase in probability by a factor of $\sim 5 \times 10^9$ when considering the entire sequence (Figure
268 4B). Like ArDCA, GENERALIST-based local optima were significantly more conservative. As seen
269 in Figure 4A, the local optimum sequences differed from the closest naturally occurring
270 sequences on an average by 8%. As seen in Figure 4B, the per amino acid improvement was
271 only ~ 1.1 fold with a total average increase in probability by a factor of $\sim 7 \times 10^2$ when
272 considering the entire sequence.

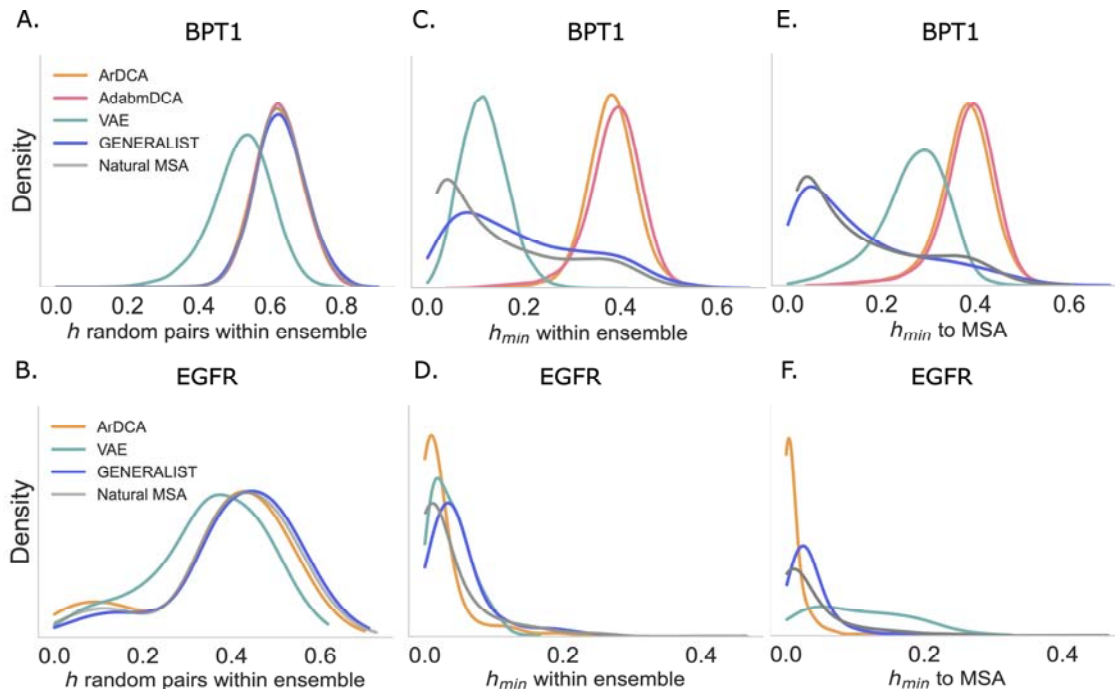
273
274 To test whether these sequences potentially fold in stable 3D structures, we used AlphaFold2²²,
275 a recent machine learning method that can predict 3D structures from sequences and MSAs (SI
276 Section 6). We used the sequence-averaged predicted local distance difference test (plddt) as a
277 proxy for quality of predicted structures. Previous studies have shown that a sequence average
278 plddt of > 80 corresponds to sequences that are likely to fold in stable 3D structures²³. As seen
279 in Figure 4C, local optimal sequences imputed by adabmDCA were predicted to be significantly
280 worse folders compared to both GENERALIST and ArDCA. While ArDCA and GENERALIST produce
281 sequences that were predicted to be comparable by AlphaFold2 on average.

282

283 These results show that GENERALIST can identify local optima in the sequence space. These
284 optima are typically not seen in nature. The optimal sequences predicted by GENERALIST were
285 also predicted by AlphaFold2 to fold in stable 3D structures

286

287 **GENERALIST reproduces statistics related to the density of sequences in the natural ensemble**
288



289
290 **Figure 5. Panels A and B.** Distribution of fractional Hamming distances between random pairs of
291 sequences within an ensemble shown for BPT1 (panel A) and EGFR (panel B). **Panels C and D.** Distribution
292 of fractional Hamming distances to the closest sequence within an ensemble for different models shown
293 for BPT1 (panel C) and EGFR (panel D). **Panels E and F.** Distribution of fractional Hamming distances to
294 closest natural sequence for different models shown for BPT1 (panel E) and EGFR (panel F).
295

296 In addition to reproducing the summary statistics (Figure 3), an important test for generative
297 models is capturing the density of sequences in the natural ensemble^{7,24}. To that end, we
298 evaluated three different statistics for all generated ensembles: (a) the distribution of distances
299 between pairs of randomly picked sequences, (b) the distribution of nearest neighbor distances,
300 and (c) the distribution of distances to the nearest natural neighbor.

301

302 In Figure 5A and 5B (SI Figure 5), we plot the distribution of fractional Hamming distances
303 between pairs of random sequences in an ensemble. We see that all generative models, except
304 for the VAEs, accurately reproduced this distribution, implying that most ensembles captured

305 the expanse of the natural sequence ensemble. Ensembles generated using VAEs comprised
306 sequences that are on average closer to each other than natural sequences.

307

308 The distribution of nearest neighbor distances portrayed a more complex picture. In Figure 5C
309 and 5D (SI Figure 6, SI Section 2), we plot the distribution of fractional Hamming distances to the
310 nearest neighbor within the ensemble. When MSAs were large (BPT1 in Figure 5C and DHFR in SI
311 Figure 6), ArDCA/adabmDCA generated ensemble comprised sequences that were farther away
312 from each other compared to natural sequences. In contrast, for small MSAs (EGFR in Figure 5D
313 and p53 and mTor in SI Figure 6), ArDCA generated ensembles comprised sequences that were
314 closer to each other compared to natural sequences. VAEs generated ensemble always
315 comprised sequences that were on average closer to each other than natural sequences (with
316 the exception of mTor). In contrast GENERALIST generated ensemble closely reproduced the
317 density of nearest neighbor sequences observed in the natural ensembles.

318

319 Next, we compared the distance distribution to the nearest natural neighbor. Here too,
320 GENERALIST generated ensembles closely reproduced the density of nearest neighbor
321 sequences (Figure 5E and 5F, SI Figure 7). In contrast, ArDCA/adabmDCA generated sequences
322 were farther from the natural sequences if the MSA was large (BPT1 in Figure 5E and DHFR in SI
323 Figure 7). ArDCA generated ensembles for proteins with small MSAs were overfit to the MSA as
324 evidenced by a distribution of distances with a sharp peak at zero (EGFR in Figure 5F and p53
325 and mTor in SI Figure 7). This overfitting also explains the accuracy with which ArDCA can
326 reproduce sequence summary statistics for EGFR and other large proteins with small MSAs
327 (Figure 3F, SI Figure 3). Finally, VAEs generated ensemble comprised sequences that were
328 farther away compared to natural sequences for all proteins.

329

330 These results show that an optimally tuned GENERALIST ensemble can capture various aspects
331 of the density of sequences in the natural ensemble.

332

333 **Discussion**

334

335 Generative models of protein sequence families are an important tool for protein scientists and
336 engineers alike. Ideally, these models should be simple to learn, tunable, and accurate,

337 especially when studying proteins of significant clinical interest which tend to be large proteins
338 with small MSAs.

339

340 In this work, we examined three state-of-the-art models. Physics-based Potts models could only
341 be used to model small sequences, limiting their application to single domains and small
342 proteins. Moreover, these models could not be tuned. The sequence ensemble generated by
343 Potts models could not reproduce the density of sequences in the natural ensemble and had
344 optima that appeared unnatural. In contrast, the autoregressive generalization of the Potts
345 model was significantly more efficient in model fitting and more accurate in reproducing
346 summary statistics such as frequencies of higher order amino acid combinations (Figure 3). The
347 model also reproduced reasonable local optima that were computationally deemed to fold in
348 stable 3D structures (Figure 4). However, the autoregressive Potts model could not reproduce
349 the density of sequences in the natural ensemble (Figure 5). Importantly, given that the model
350 has $O(L^2)$ parameters for proteins of sequence length L , this model overfits the training data
351 when modeling human proteins of significant clinical interest which are large and have small
352 MSAs.

353

354 Neural networks based variational autoencoders were efficient and did not appear to overfit the
355 training data (Figure 5). Overall, these models were less accurate in predicting summary
356 statistics of sequences compared to GENERALIST, the Potts model, and the autoregressive
357 generational of the Potts model. At the same time, potentially owing to model complexity (and
358 therefore parameter non-identifiability) and low amounts of training data, the models appeared
359 to not have any systematic trends with respect to accuracy and overfit as a function of the
360 dimension of the latent space.

361

362 In contrast, GENERALIST is efficient, accurate, and tunable, allowing us to analyze large proteins
363 with small MSAs. Notably, given its simple structure, there are several avenues of improving
364 GENERALIST. For example, function/fitness information obtained from deep mutational
365 scanning¹⁵ can be incorporated as constraints on the energies and phylogenetic information can
366 be imposed as constraints on the latent space. Finally, GENERALIST can be easily reformulated
367 for any other categorical data, for example, presence/absence of single nucleotide

368 polymorphisms or nucleotide sequences. We believe that GENERALIST will be an asset for
369 protein scientists and engineers alike.

370

371

372 Acknowledgments

373 HA, BE, and PD are supported by NIGMS grant R35GM142547. The authors would like to thank
374 Francesco Zamponi and Martin Weigt for fruitful discussions about implementation of the Potts
375 model and the autoregressive Potts model. We would like to thank Juannan Zhou for critical
376 comments and useful discussions.

377

378 References

379

- 380 1. Povolotskaya, I. S. & Kondrashov, F. A. Sequence space and the ongoing expansion of the
381 protein universe. *Nature* **465**, 922–926 (2010).
- 382 2. Zeldovich, K. B., Chen, P. & Shakhnovich, E. I. Protein stability imposes limits on organism
383 complexity and speed of molecular evolution. *Proc. Natl. Acad. Sci.* **104**, 16152–16157 (2007).
- 384 3. Fraser, H. B., Wall, D. P. & Hirsh, A. E. A simple dependence between protein evolution rate
385 and the number of protein-protein interactions. *BMC Evol. Biol.* **3**, 11 (2003).
- 386 4. Konaté, M. M. *et al.* Molecular function limits divergent protein evolution on planetary
387 timescales. *eLife* **8**, e39705 (2019).
- 388 5. Cocco, S., Feinauer, C., Figliuzzi, M., Monasson, R. & Weigt, M. Inverse statistical physics of
389 protein sequences: a key issues review. *Rep. Prog. Phys.* **81**, 032601 (2018).
- 390 6. Levy, R. M., Haldane, A. & Flynn, W. F. Potts Hamiltonian models of protein co-variation, free
391 energy landscapes, and evolutionary fitness. *Curr. Opin. Struct. Biol.* **43**, 55–62 (2017).
- 392 7. Barrat-Charlaix, P., Muntoni, A. P., Shimagaki, K., Weigt, M. & Zamponi, F. Sparse generative
393 modeling via parameter reduction of Boltzmann machines: Application to protein-sequence
394 families. *Phys. Rev. E* **104**, 024407 (2021).
- 395 8. Mann, J. K. *et al.* The Fitness Landscape of HIV-1 Gag: Advanced Modeling Approaches and
396 Validation of Model Predictions by In Vitro Testing. *PLoS Comput. Biol.* **10**, e1003776 (2014).
- 397 9. Muntoni, A. P., Pagnani, A., Weigt, M. & Zamponi, F. adabmDCA: adaptive Boltzmann
398 machine learning for biological sequences. *BMC Bioinformatics* **22**, 528 (2021).
- 399 10. Thul, P. J. & Lindskog, C. The human protein atlas: A spatial map of the human
400 proteome. *Protein Sci. Publ. Protein Soc.* **27**, 233–244 (2018).
- 401 11. Barton, J. P., Cocco, S., De Leonardis, E. & Monasson, R. Large pseudocounts and L2-
402 norm penalties are necessary for the mean-field inference of Ising and Potts models. *Phys.*
403 *Rev. E Stat. Nonlin. Soft Matter Phys.* **90**, 012132 (2014).
- 404 12. Rodriguez Horta, E., Barrat-Charlaix, P. & Weigt, M. Toward Inferring Potts Models for
405 Phylogenetically Correlated Sequence Data. *Entropy* **21**, 1090 (2019).
- 406 13. Chen, W.-C., Zhou, J., Sheltzer, J. M., Kinney, J. B. & McCandlish, D. M. Field-theoretic
407 density estimation for biological sequence space with applications to 5' splice site diversity
408 and aneuploidy in cancer. *Proc. Natl. Acad. Sci.* **118**, e2025782118 (2021).
- 409 14. Trinquier, J., Uguzzoni, G., Pagnani, A., Zamponi, F. & Weigt, M. Efficient generative
410 modeling of protein sequences using simple autoregressive models. *Nat. Commun.* **12**, 5800
411 (2021).

412 15. Strokach, A. & Kim, P. M. Deep generative modeling for protein design. *Curr. Opin. Struct. Biol.* **72**, 226–236 (2022).

413 16. Burgin, C. J., Colella, J. P., Kahn, P. L. & Upham, N. S. How many species of mammals are there? *J. Mammal.* **99**, 1–14 (2018).

414 17. Dixit, P. D. Thermodynamic inference of data manifolds. *Phys. Rev. Res.* **2**, 023201 (2020).

415 18. Zhao, X., Plata, G. & Dixit, P. D. SiGMoID: A super-statistical generative model for binary data. *PLOS Comput. Biol.* **17**, e1009275 (2021).

416 19. Hawkins-Hooker, A. *et al.* Generating functional protein variants with variational autoencoders. *PLOS Comput. Biol.* **17**, e1008736 (2021).

417 20. McGee, F. *et al.* The generative capacity of probabilistic protein sequence models. *Nat. Commun.* **12**, 6302 (2021).

418 21. Hertz, J., Krogh, A. & Palmer, R. G. *Introduction to the Theory of Neural Computation*. (CRC Press, 2018). doi:10.1201/9780429499661.

419 22. Jumper, J. *et al.* Highly accurate protein structure prediction with AlphaFold. *Nature* **596**, 583–589 (2021).

420 23. David, A., Islam, S., Tankhilevich, E. & Sternberg, M. J. E. The AlphaFold Database of Protein Structures: A Biologist’s Guide. *J. Mol. Biol.* **434**, 167336 (2022).

421 24. Yelmen, B. *et al.* Creating artificial human genomes using generative neural networks. *PLOS Genet.* **17**, e1009303 (2021).

432